

# Direct evidence of Kerr-like nonlinearity by femtosecond Z-scan technique

Wei-Qiang He, Chun-Ming Gu\*, and Wen-Zhong Shen

Laboratory of Condensed Matter Spectroscopy and Opto-Electronic Physics,  
Department of Physics, Shanghai Jiao Tong University,  
1954 Hua Shan Road, Shanghai 200030, P. R. China  
[cmgu@sjtu.edu.cn](mailto:cmgu@sjtu.edu.cn)

**Abstract:** Kerr-like nonlinearity  $n_2^{\text{THz}}$  induced via terahertz (THz) radiation and linear electro-optic (EO) effect is investigated in (110), (111) and (100) oriented ZnTe crystals using Z-scan technique with femtosecond laser pulses. We have proposed a model, taking into account the Kerr-like nonlinearity  $n_2^{\text{THz}}$ , to describe well the experimental incident polarization dependence of the nonlinear refractive index  $n_2$ . It is found that for a (110) ZnTe crystal the nonlinear refractive index  $n_2$  is dominated by the Kerr-like nonlinearity  $n_2^{\text{THz}}$ , while  $n_2$  in the (111) ZnTe crystal mainly comes from the combined contributions of the Kerr-like nonlinearity  $n_2^{\text{THz}}$  and conventional Kerr nonlinearity  $n_2^{\text{Kerr}}$ . We also show strong two-photon absorption (TPA) anisotropy and crystal orientation dependence of TPA in ZnTe crystals.

©2006 Optical Society of America

**OCIS codes:** (190.3270) Kerr effect; (160.2100) Electro-optical materials; (320.2250) Femtosecond phenomena

---

## References

1. J. P. Caumes, L. Videau, C. Rouyer, and E. Freysz, "Kerr-Like Nonlinearity Induced via Terahertz Generation and the Electro-Optical Effect in Zinc Blende Crystals," *Phys. Rev. Lett.* **89**, 047401 (2002).
2. S. Wu, Z. Q. Ren, W. Z. Shen, H. Ogawa, and Q. X. Guo, "Effects of dry etching processes on effective refractive index of ZnTe surface layers in terahertz region," *J. Appl. Phys.* **94**, 3800-3804 (2003).
3. B. B. Hu, X. C. Zhang, D. H. Auston, and P. R. Smith, "Free-space radiation from electro-optic crystals," *Appl. Phys. Lett.* **56**, 506-508 (1990).
4. L. Xu, X. C. Zhang, and D. H. Auston, "Terahertz beam generation by femtosecond optical pulses in electro-optic materials," *Appl. Phys. Lett.* **61**, 1784-1786 (1992).
5. Y. R. Shen, "Far-infrared generation by optical mixing," *Prog. Quantum Electron.* **4**, 207-232 (1976).
6. A. Bonvalet, M. Joffre, J. L. Martin, and A. Migus, "Generation of ultrabroadband femtosecond pulses in the mid-infrared by optical rectification of 15 fs light pulses at 100 MHz repetition rate," *Appl. Phys. Lett.* **67**, 2907-2909 (1995).
7. A. Nahata, A. S. Weling, and T. F. Heinz, "A wideband coherent terahertz spectroscopy system using optical rectification and electro-optic sampling," *Appl. Phys. Lett.* **69**, 2321-2323 (1996).
8. X. C. Zhang, B. B. Hu, and J. T. Darrow, "Generation of femtosecond electromagnetic pulses from semiconductor surfaces," *Appl. Phys. Lett.* **56**, 1011-1013 (1990).
9. P. N. Saeta, and B. I. Greene, "Short terahertz pulses from semiconductor surfaces: The importance of bulk difference-frequency mixing," *Appl. Phys. Lett.* **63**, 3482-3484 (1993).
10. Q. Chen, M. Tani, Z. P. Jiang, and X. C. Zhang, "Electro-optic transceivers for terahertz-wave applications," *J. Opt. Soc. Am. B* **18**, 832-831 (2001).
11. X. C. Zhang, Y. Jin, and X. F. Ma, "Coherent measurement of THz optical rectification from electro-optic crystals," *Appl. Phys. Lett.* **61**, 2764-2766 (1992).
12. A. Rice, Y. Jin, X. F. Ma, X. C. Zhang, D. Bliss, J. Larkin, and M. Alexander, "Terahertz optical rectification from <110> zinc-blende crystals," *Appl. Phys. Lett.* **64**, 1324-1326 (1994).
13. M. Sheik-Bahae, A. A. Said, and E. W. Van Stryland, "High-sensitivity, single-beam  $n_2$  measurements," *Opt. Lett.* **14**, 955-957 (1989).
14. M. Sheik-Bahae, A. A. Said, T. H. Wei, D. J. Hagan, and E. W. Van Stryland, "Sensitive measurement of optical nonlinearities using a single beam," *IEEE J. Quantum Electron.* **26**, 760-769 (1990).
15. R. DeSalvo, D. J. Hagan, M. Sheik-Bahae, G. Stegeman, and E. W. Van Stryland, "Self-focusing and self-defocusing by cascaded second-order effects in KTP," *Opt. Lett.* **17**, 28-30 (1992).

16. M. L. Sundheimer, Ch. Bosshard, E. W. Van Stryland, G. I. Stegeman, and J. D. Bierlein, "Large nonlinear phase modulation in quasi-phase-matched KTP waveguides as a result of cascaded second-order processes," *Opt. Lett.* **18**, 1397-1399 (1993).
17. Ch. Bosshard, R. Spreiter, M. Zgonik, and P. Gunter, "Kerr Nonlinearity via Cascaded Optical Rectification and the Linear Electro-optic Effect," *Phys. Rev. Lett.* **74**, 2816-2819 (1995).
18. I. Biaggio, "Nonlocal Contributions to Degenerate Four-Wave Mixing in Noncentrosymmetric Materials," *Phys. Rev. Lett.* **82**, 193-196 (1999).
19. M. Yin, H. P. Li, S. H. Tang, and W. Ji, "Determination of nonlinear absorption and refraction by single Z-scan method," *Appl. Phys. B* **70**, 587-591 (2000).
20. A. A. Said, M. Sheik-Bahae, D. J. Hagan, T. Wei, J. Wang, J. Young, and E. W. Van Stryland, "Determination of bound-electronic and free-carrier nonlinearities in ZnSe, GaAs, CdTe, and ZnTe," *J. Opt. Soc. Am. B* **9**, 405-413 (1992).
21. R. DeSalvo, M. Sheik-Bahae, A. A. Said, D. J. Hagan, and E. W. Van Stryland, "Z-scan measurements of the anisotropy of nonlinear refraction and absorption in crystals," *Opt. Lett.* **18**, 194-196 (1993).
22. D. C. Hutchings, and B. S. Wherrett, "Theory of anisotropy of two-photon absorption in zinc-blende semiconductors," *Phys. Rev. B* **49**, 2418-2426 (1994).
23. M. Murayama, and T. Nakayama, "Symmetry-induced anisotropy of two-photon absorption spectra in zinc-blende semiconductors," *Phys. Rev. B* **55**, 9628-9636 (1997).

## 1. Introduction

Materials with large optical Kerr-like nonlinearity are essential for future optical device applications in all-optical switches, optical limiters and waveguide formation. Besides the intrinsic Kerr nonlinearity possessed in all materials, there is another important contribution that occurs only in electro-optic (EO) media during the generation of terahertz (THz) radiation. This contribution can provide an efficient alternative for creating equivalent Kerr-like nonlinearity, which could produce a similar nonlinear refractive index  $n_2$ , noted  $n_2^{\text{THz}}$ . Such effects were first reported in [1], they evidenced this kind of Kerr-like nonlinearity resulting from the propagation of a THz radiation in a zinc blende crystal with a heterodyne Kerr effect setup, and demonstrated its competition with a third-order optical Kerr effect. In general, it is difficult to quantitative analyze this new contribution of  $n_2^{\text{THz}}$  to  $n_2$  alone in media since a contribution from intrinsic Kerr nonlinearity will also occur at the same time. Moreover, the contribution from  $n_2^{\text{THz}}$  is adjustable in sign and amplitude. Until now, no theoretical and experimental data to our knowledge is available to both the sign and magnitude of the Kerr-like nonlinearity  $n_2^{\text{THz}}$ .

On the other hand, ZnTe, as the primary EO crystal of THz radiation in both emission and detection [2], has been extensively investigated from both fundamental and applied point view [3-7]. Though the nonlinear optical process that occurs in conditions of THz excitation has not been fully discussed, it is widely accepted that the second-order optical rectification is the major process that generates THz radiation [8, 9]. Based on this theory, Chen *et al.* [10] have shown a detailed theoretical description of the crystal-orientation-dependent generation and detection of THz radiation by (110) and (111) zinc blende EO crystals, and indicated that (110) zinc blende crystal has a relative larger THz radiation efficiency than that of (111) zinc blende crystal. Moreover, authors in [11, 12] indicated that no radiated THz signal is observed from (100) zinc blende crystal under the condition of normal optical incidence. The characteristic of the crystal-orientation-dependent efficiency as well as incident-polarization-dependent THz generation in ZnTe crystals offers the possibility to distinguish two nonlinear optical mechanisms even when they are present simultaneously.

Z-scan is a simple but sensitive single-beam method to determine both the sign and magnitude of nonlinear refractive index as well as nonlinear absorption coefficient of a given material. In this paper, rather than using a complex heterodyne Kerr effect experimental arrangement employed in [1], by performing the single-beam Z-scan with femtosecond laser pulses on (110), (111) and (100) oriented ZnTe crystals, we present the experimental evidence of this new kind of Kerr-like nonlinearity induced via THz generation and the linear EO effect in the media. In addition, we present a quantitative analysis of the incident polarization

dependence of  $n_2$  in the three samples taking into account the contribution of  $n_2^{\text{THz}}$ . Finally, we show strong TPA anisotropy and crystal orientation dependence of TPA in ZnTe crystals.

## 2. Experiment

Our experiments are performed in commercial bulk (110), (111) and (100) oriented ZnTe crystals (from company of RMT, Russia), which are all mechanically polished with 0.05  $\mu\text{m}$  aluminum and 1 mm in thickness. Bulk ZnTe crystal is a direct band gap II-VI semiconductor with a wide band gap of 2.26 eV at 300 K and a cubic zinc blende structure, therefore, besides the third-order nonlinear susceptibility  $\chi^{(3)}$ , symmetry allowed in all materials, it also has only one independent non null second-order tensor elements of  $\chi^{(2)}$  coefficient, namely  $d_{14}=d_{25}=d_{36}$ .

The experimental setup was based on a mode-locked Ti: sapphire laser, which produces laser pulses of about 100 fs duration with 82 MHz repetition rate, and 790 nm center wavelength. The Gaussian laser beam passed first through a half-wave plate, allowing us to rotate its polarization, and then the measurement was performed using standard Z-scan technique [13, 14] with a 7 cm focal-length objective lens. The peak power of the laser pulse at the focus plane is about 5.8  $\text{GW}/\text{cm}^2$  with a beam waist radius of about 11.5  $\mu\text{m}$ . The total power of the transmitted beam as well as the power in its central part was measured in the far field as functions of the sample position along the beam axis Z. These measurements corresponded to the standard open aperture (OA) and closed aperture (CA) Z-scan curves.

To accurately determine the nonlinearities in samples, a low energy scan which can be considered as the background signal is utilized to eliminate the parasitic effects due to surface roughness or sample non-uniformity [14]. It should be pointed out that, on femtosecond time scales, the thermal lens effect and the free-carriers refraction and absorption associated with the accumulation of two-photon absorption generated free carriers in media can be negligible.

## 3. Results and discussion

In general, the modification of the index of refraction  $n$  in media can be defined as  $n=n_0+n_2I$ , where  $n_0$  is the linear refractive index,  $n_2$  is the nonlinear refractive index and  $I$  is the intensity of the incoming beam. In centrosymmetric media the third-order susceptibility  $\chi^{(3)}$  is the predominant contribution to the nonlinear refractive index  $n_2$ , noted  $n_2^{\text{Kerr}}$ . However, besides the intrinsic third-order Kerr nonlinearity possessed in all materials, some noncentrosymmetric media exhibit Kerr-like nonlinearity induced by the complicated second-order optical nonlinear processes, which could give rise to a similar nonlinear refractive index  $n_2$ . For instance, cascaded second-order nonlinear effects due to second-harmonic generation (SHG) of the incident beam and other parametric processes can lead to an effective Kerr-like nonlinearity [15, 16], noted  $n_2^{\text{SHG}}$ . Moreover, Bosshard *et al.* [17] and Biaggio [18] have shown another type of Kerr-like nonlinearity via cascaded optical rectification (OR) and linear EO effect in media, noted  $n_2^{\text{OR}}$ .

Besides, it is important to note that, under the conditions of the normal incident femtosecond laser pulses with 790 nm wavelength, (110) and (111) ZnTe crystals can generate THz radiation. This THz fields can then react on the incident beam through a refractive index change produced by the linear EO effect. The combined processes of THz generation and linear EO effect can result in the modification of the nonlinear refractive index  $n_2$  in media, noted  $n_2^{\text{THz}}$ .

Taking into account all the contributions mentioned above, the nonlinear refractive index  $n_2$  of ZnTe crystals is therefore given by

$$n_2 = n_2^{\text{Kerr}} + n_2^{\text{SHG}} + n_2^{\text{OR}} + n_2^{\text{THz}} \quad (1)$$

In practice, one needs to construct different experimental setup to evaluate the sign and magnitude of each contribution. When we use single-beam Z-scan technique with a femtosecond laser pulses for measuring the nonlinear refractive index  $n_2$  in media, the measured values of  $n_2$  are the total contributions of these effects. However, Caumes *et al.* [1] clearly indicate that  $n_2^{\text{Kerr}}$  always overcomes the contribution of  $n_2^{\text{SHG}}$  and  $n_2^{\text{OR}}$  in the ZnTe

crystals and the contribution from terms of  $n_2^{\text{SHG}}$  and  $n_2^{\text{OR}}$  is negligible. Thus we can attribute the values of  $n_2$  measured with our femtosecond Z-scan technique mainly to the sum of  $n_2^{\text{Kerr}}$  and  $n_2^{\text{THz}}$ .

It is noted that the change of the nonlinear refractive index due to  $n_2^{\text{Kerr}}$  is associated with the third-order nonlinear susceptibility  $\chi^{(3)}$  whereas the Kerr-like nonlinearity  $n_2^{\text{THz}}$  is proportional to intensity of THz radiation. Thus by performing the Z-scan on ZnTe crystals with different THz radiation efficiencies the contribution of the two processes could be easily separated.

### 3.1 Z-scan results

Fig. 1 shows the results of CA Z-scan trace (with background signal subtracted) performed on 1-mm-thick (110), (111) and (100) oriented ZnTe crystals at one particular optical beam intensity. As can be seen from the Fig., around the position of the beam waist ( $z=0$ ) a valley to peak signature is not obvious, which indicates the presence of strong two-photon absorption in samples. Following the same procedure described in [19], we can separate the contributions from the nonlinear refraction and two-photon absorption (TPA) from a single CA Z-scan curve, corresponding to OA and CA/OA trace as shown in Fig. 1. The shape of the CA/OA trace is indicative of positive (self-focusing) nonlinearity. The solid lines in the Fig. represent theoretical fittings obtained with the parameters  $n_2=7.1\times 10^{-18}$  m<sup>2</sup>/W,  $\beta=7.3$  cm/GW for a (110) sample,  $n_2=5.4\times 10^{-18}$  m<sup>2</sup>/W,  $\beta=6.2$  cm/GW for a (111) sample, and  $n_2=4.7\times 10^{-18}$  m<sup>2</sup>/W,  $\beta=5.1$  cm/GW for a (100) sample, respectively. In a similar experimental conditions, the authors [19] have reported the Kerr nonlinearities of ZnSe ( $n_2=2.4\times 10^{-18}$  m<sup>2</sup>/W) and CdS ( $n_2=3.6\times 10^{-18}$  m<sup>2</sup>/W) crystals. Both of them have the same zinc blende structure as ZnTe crystals, but no THz radiation was generated in the media. Our measured values  $n_2$  for ZnTe are of the same order of the magnitude but a slightly larger than the reported data [19] for ZnSe and CdS.

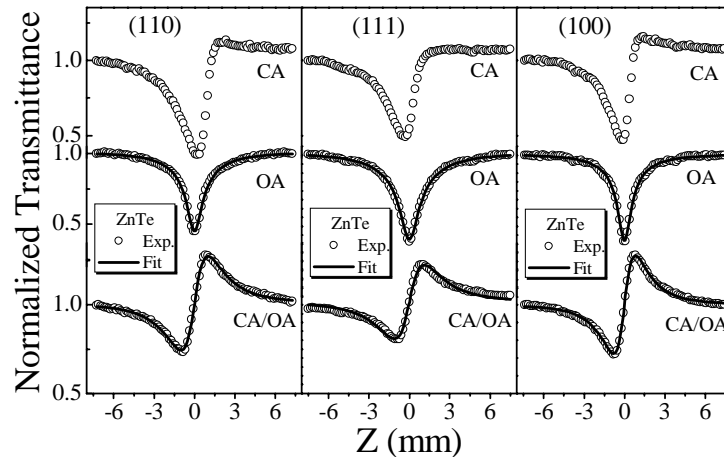


Fig. 1. Z-scan curves (closed aperture (CA) and open aperture (OA)) of (110), (111) and (100) oriented ZnTe crystals measured with femtosecond laser pulses at 790 nm, respectively. The solid lines are fitting curves.

As we can see, there is a large difference between the data obtained under the same experimental conditions for the three samples, especially the value of  $n_2$  in (110) sample is 1.5 times larger than that in (100) sample. In addition, the value of  $n_2$  in (111) sample is smaller than that in (110) sample and slightly larger than that in (100) sample. We attribute this difference to the influence of the Kerr-like nonlinearity  $n_2^{\text{THz}}$ . Considering the fact of different THz radiation efficiencies in the samples, we can further estimate that the Kerr-like effects increase the measured  $n_2$  value demonstrating  $n_2^{\text{THz}}$  has positive sign, and increase of THz radiation efficiency would result in larger  $n_2$  values due to the contribution of  $n_2^{\text{THz}}$ .

### 3.2 Incident polarization dependence of $n_2$

For further proving the role of this kind of Kerr-like nonlinearity  $n_2^{\text{THz}}$  in the nonlinear refractive index  $n_2$  during the generation of THz radiation, the normal incident polarization dependence of  $n_2$  are measured at the same input intensity in (110), (111) and (100) ZnTe crystals. Fig. 2 shows the experimental (filled squares)  $n_2$  as a function of the polarization direction of normal incidence for the three samples with different surface orientations, which clearly reveals the general tendency of  $n_2$  values between the three samples. The measured  $n_2$  value in (111) sample is smaller than that in (110) sample and slightly larger than that in (100) sample for the whole angular range. Note that THz radiation efficiency of (111) ZnTe crystal is lower than that of (110) ZnTe crystal and higher than that of (100) ZnTe crystal. At the same incident intensity, an increase of THz radiation efficiency would increase the intensity of THz radiation in the sample, thus eventually raises the contribution of the Kerr-like refraction signal. Therefore, Effect of increase of THz radiation efficiency on the total nonlinear refractive index is thus probed. Besides, the different shapes of the nonlinear refractive index  $n_2$  curves for the three samples are related to incident polarization dependence of THz radiation, and the details of calculations for estimation of the Kerr-like nonlinearity  $n_2^{\text{THz}}$  in the three samples are given as follows.

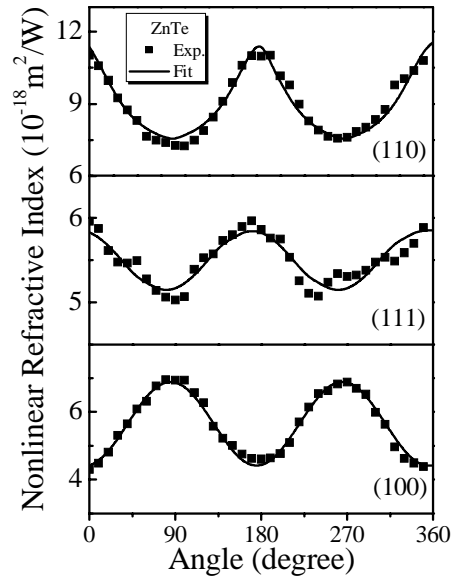


Fig. 2. Angular dependence of the nonlinear refractive index as a function of the normally incident polarization angle for (110), (111) and (100) ZnTe crystals, respectively.

For (100) ZnTe crystal, theoretical and experimental studies indicate that there is no radiated THz signal from (100) zinc blende at normal incidence [11, 12]. Hence, at normal incidence the nonlinear refractive index  $n_2$  in the (100) sample is mainly due to conventional Kerr nonlinearity  $n_2^{\text{Kerr}}$  only. If we define a laboratory coordinate system ( $x$ ,  $y$ ,  $z$ ) with  $x$  parallel to the optical table,  $y$  perpendicular to the optical table and  $z$  along the direction of optical propagation, due to the symmetry of refractive ellipse, the nonlinear refractive index  $n_2$  can be simply described as

$$n_2 = n_2^{\text{Kerr}} \propto A + B \cos(2\theta) \quad (2)$$

where  $\theta$  is the angle between the  $y$  axis and the polarization direction of incidence, and  $A$  and  $B$  are the constants associated with  $\chi^{(3)}$ .

The fits to Eq. (2) are shown as the solid lines in Fig. 2 for (100) ZnTe crystal and quite acceptable. The good agreement indicates that, under the condition of normal incidence, the

Kerr nonlinearity  $n_2^{\text{Kerr}}$  due to  $\chi^{(3)}$  is the major nonlinear process that induces nonlinear refractive index  $n_2$  in (100) ZnTe crystal.

For (110) and (111) ZnTe crystals, THz radiation has been studied in detail by Chen *et al.* [10]. They find that the angular dependence of the magnitude of the THz electric fields and its direction from (110) ZnTe are given by the following expressions

$$|E_{\text{THz}}| \propto |P| = d_{14} E_0^2 \left[ \sin^2 \theta (1 + 3 \cos^2 \theta) \right]^{1/2} \quad (3)$$

$$\tan \phi = 2 \cot \theta \quad (4)$$

where  $\theta$  is the angle between the polarization of the optical beam and the y axis,  $\phi$  is defined as the angle of the polarization of THz fields with respect to the y axis,  $d_{14}$  is the non-vanishing second-order nonlinear optical coefficient, and  $E_0$  is the amplitude of electric fields of the incidence.

The polarization of THz radiation is always linear and its polarization direction depends on  $\theta$  as what we can see from the above equations. This THz fields can induce a refractive-index ellipsoid in the crystal via the linear EO effect, and the main axes of the ellipsoid are  $\theta$  dependence. By use of above Eqs. (3) and (4), together with linear EO effect theory we deduce that the angular dependence of the nonlinear refractive index  $n_2^{\text{THz}}$  induced by THz radiation and linear EO effect can be written as

$$n_2^{\text{THz}}(\theta) \propto \sin \theta (1 + 3 \sin^2 \phi)^{1/2} \left[ \cos \phi + (1 + 3 \sin^2 \phi)^{1/2} \cos 2(\theta - \phi) \right] \quad (5)$$

with  $\tan 2\phi = -\cot \theta$ .

where  $\phi$  is the angle between the direction of the main axes of the refractive-index ellipse and the y axis.

In Fig. 2 we plot the calculated results (solid line) of the polarization dependence of  $n_2$  using Eq. (5) for (110) sample. A fairly good agreement between the calculated curve and the experimental data is clearly demonstrated, revealing that the model, neglecting the contribution of  $n_2^{\text{Kerr}}$ , can be successfully applied to describe the polarization dependence of  $n_2$  in (110) sample. At the same time, through this model, we can conclude that the contribution of  $n_2^{\text{Kerr}}$  is negligible to the total nonlinear refractive index  $n_2$  under the experimental conditions. Thus the Kerr-like nonlinearity  $n_2^{\text{THz}}$  due to the combined processes of THz generation and linear EO effect is the dominant mechanism of nonlinearity.

In a similar calculation, for (111) ZnTe crystal, the angular dependence of nonlinear refractive index  $n_2^{\text{THz}}$  can be decided by

$$n_2^{\text{THz}}(\theta) \propto -\frac{\cos 2\theta}{3\sqrt{6}} + \frac{1}{2} \left( \frac{32}{27} + \frac{40}{27} \sin^2 2\theta \right)^{1/2} \cos 2(\theta - \phi) \quad (6)$$

where  $\phi$  is decided by  $\tan 2\phi = 1.5 \tan 2\theta$ .

If we only use Eq. (6) to fit our experimental data, the fitting results are quite unacceptable. A good fitting with the experimental data shown in Fig. 2 is found only by using Eqs. (2) and (6). Here we assume the contribution of  $n_2^{\text{Kerr}}$  to  $n_2$  arising from  $\chi^{(3)}$  is the same for (100) and (111) crystal. The excellent fitting trace indicates that the nonlinear refractive index  $n_2$  is mainly attributed to the combined contributions of both  $n_2^{\text{THz}}$  and  $n_2^{\text{Kerr}}$ , and  $n_2^{\text{Kerr}}$  cannot be neglected compared to  $n_2^{\text{THz}}$ . This conclusion is very reasonable. Considering the fact that THz radiation efficiency of (111) ZnTe crystal is lower than that of (110) ZnTe crystal [10]. Reduction of the intensity of the generated THz radiation in the sample would result in decrease of the contribution of the Kerr-like refraction signal. Therefore, for smaller THz radiation efficiency of the sample the influence of the Kerr-like nonlinearity in the total nonlinear refraction signal would reduce. Accordingly, the contribution from  $n_2^{\text{Kerr}}$  is comparable with the total value of  $n_2$ , the magnitude of  $n_2$  in (111) sample eventually involves the contribution from Kerr-like nonlinearity as well as that from third-order Kerr nonlinearity.

Based on the above discussion, we know the large discrepancies between the total nonlinear refractive indices  $n_2$  for the three crystal orientations clearly reveal the evolution of  $n_2$  due to the competition between  $n_2^{\text{THz}}$  and  $n_2^{\text{Kerr}}$ , which is consistent with the conclusion in [1]. Theoretically, the maximum magnitude of the generated THz fields from (111) ZnTe is

only 70.7% of that from (110) ZnTe, and there is no THz signals from (100) crystal [10-12]. Moreover, the Kerr-like nonlinearity  $n_2^{\text{THz}}$  is not only proportional to intensity of THz radiation, but also related to the generated THz radiation polarization. Thus, by performing the Z-scan on three crystals with different orientations, the contribution of the Kerr-like nonlinearity  $n_2^{\text{THz}}$  to  $n_2$  is clearly verified, furthermore we present quantitative analysis of the Kerr-like nonlinearity  $n_2^{\text{THz}}$  and determine the positive sign of  $n_2^{\text{THz}}$ . Here, it should be noted that the intrinsic  $n_2^{\text{Kerr}}$  contribution to  $n_2$  can only give rise to a small difference between the three crystal orientations since  $n_2^{\text{Kerr}}$  is associated with the third-order nonlinear susceptibility  $\chi^{(3)}$ .

### 3.3 Incident polarization dependence of $\beta$

When ZnTe crystal is excited by femtosecond laser pulses with the photon energy 1.57 eV below the band gap, intense fluorescence, as expected, is clearly observed especially when the sample is close to the focal plane, demonstrating the strong two-photon absorption process in the media. Large values of  $\beta$  obtained from the numerical results in Fig. 1 verified this phenomenon, and this range of values for  $\beta$  agrees well with reported data [20] within the experimental error.

In this work, we also determine the incident polarization dependence of TPA in (110), (111) and (100) ZnTe crystals, respectively. Fig. 3 shows TPA coefficient  $\beta$  of the three samples as a function of the polarization direction of normal incidence. Such a strong polarization dependence of TPA, called TPA anisotropy, is because the third-order nonlinear optical susceptibility  $\chi^{(3)}$  tensor of ZnTe crystal contains off-diagonal elements, as a consequence of which the TPA exhibits optical polarization dependence [21-23]. In addition, the discrepancy between  $\beta$  obtained in the three samples with the same incident polarization angle as shown in Fig. 3 reveals the crystal orientation dependence of the TPA coefficient.

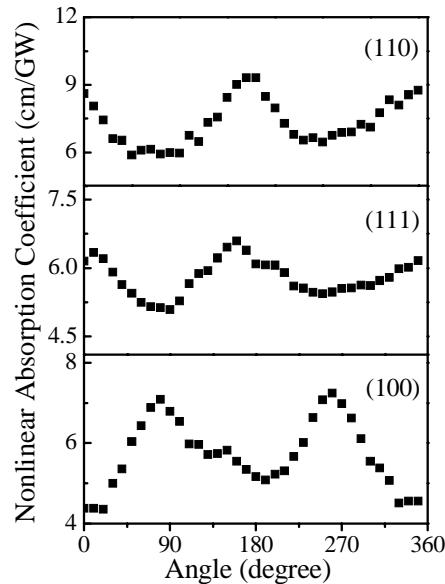


Fig. 3. Measured angular dependence of the nonlinear absorption as a function of the normally incident polarization angle for (110), (111) and (100) ZnTe crystals, respectively.

## 4. Conclusion

In summary, We have shown that there exists a large contribution of Kerr-like nonlinearity  $n_2^{\text{THz}}$  to the nonlinear refractive index  $n_2$  because of the combined processes of THz generation and linear EO effect using a simple single-beam Z-scan setup. We find that  $n_2^{\text{THz}}$  is always positive and strongly dependent on THz radiation efficiency in the media. In addition,

the model, which has been successfully applied to describe the incident polarization dependence of the nonlinear refractive index  $n_2$  in (110), (111) and (100) ZnTe crystals, respectively, is proposed to account for the Kerr-like nonlinearity  $n_2^{\text{THz}}$ . It is found that, for a (110) ZnTe crystal the nonlinear refractive index  $n_2$  is dominated by Kerr-like nonlinearity  $n_2^{\text{THz}}$ ; for a (111) ZnTe crystal both  $n_2^{\text{THz}}$  and  $n_2^{\text{Kerr}}$  is the primary contributions to the nonlinear refractive index  $n_2$  due to its relatively low THz radiation efficiency in the medium; for a (100) ZnTe crystal  $n_2^{\text{Kerr}}$  is the predominant contribution to the nonlinear refractive index  $n_2$  because of non THz generation under the normal incident in the medium.

Finally, we show the incident polarization dependence of TPA coefficient in the crystals. Large TPA coefficient values are obtained, and strong TPA anisotropy and crystal orientation dependence of TPA are observed in the ZnTe crystals. Our work is helpful to the basic physical understanding of THz generation, as well as to develop novel devices based on these nonlinearities.

### **Acknowledgments**

This work was supported in part by the Funds for Outstanding Young Researchers from the National Nature Science Foundation of China (Grant No. 10125416) and Shanghai Key Projects for Basic Research of Shanghai, China (Grant No. 03JC14082).